Acoustics 2021
Wollongong, Australia
MAKING WAVES

Sound directivity from a 250kW gas turbine exhaust system

Ben Cazzolato, Orddom Leav and Carl Howard

School of Mechanical Engineering, University of Adelaide, Australia

ABSTRACT

Experiments and numerical simulations have shown that sound radiated from vertically orientated hot exhaust stacks is strongly refracted away from the exhaust plume. In gentle cooler horizontal cross-flow, the plume bends downwards, which subsequently leads to increased refraction of the sound towards the horizontal plane downwind from the stack outlet. This paper builds upon previous research and reports on field trials of the sound directivity measured from a 250kW gas turbine (Turbine Technologies Minilab SR-30 Gas Turbine). The turbine was operated at two turbine shaft speeds, approximately 45,000RPM and 75,000RPM delivering exhaust jet flow speeds and temperatures of Mach M_j = 0.06-0.12 and T_j = 400°C-560°C, respectively, and with wind conditions ranging from calm to 8m/s. It was found that previous research could be reproduced in the field, with SPLs downwind of the exhaust stack 10-12 dB higher than spherical spreading predicts. The paper concludes with guidelines for acousticians to assist in far-field predictions of sound pressure levels arising from hot exhausts such as those found in gas turbine power plants.

1 INTRODUCTION

Open cycle gas turbines (OCGTs), also known as single cycle gas turbines, are increasingly being used for power generation as they are able to provide base loads in peaking or uncertain conditions and can respond quickly to power grid demands. It has been widely reported (Björk, 1994; Broner, 2010, 2011, 2012; Hessler, 2004, 2005; Hetzel et al., 2009; Kudernatsch, 2000; Lucas et al., 1996; Newman et al., 1980) that OCGT can lead to increased levels of low-frequency noise in communities near these plants, significantly impacting such communities when certain meteorological and operating conditions occur. It has been hypothesised (Björk, 1994; Leav et al., 2017, 2018, 2021; Zaporozhets et al., 2021) that the low-frequency noise affecting neighbouring communities is due to the sound emitted from the stack being refracted by hot turbulent exhaust gases and cross-winds. Researchers at The University of Adelaide have spent the last five years investigating the phenomenon, using both numerical methods (CFD and FEA) on the University's Phoenix supercomputer, and experiments conducted in Australia's second largest wind tunnel. Figure 1 presents the results of these simulations and experiments, which shows the predicted 3D directivity from a stack without and with flow, and the corresponding experimental validation.

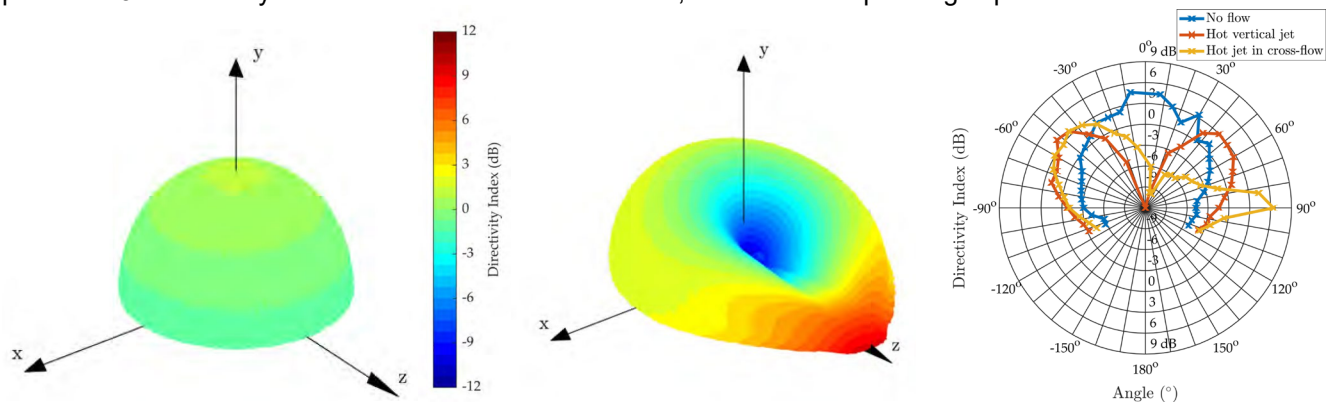

Figure 1: Predicted 3D directivity plots for sound radiation from a stack in an isothermal field (leftmost), and a heated exhaust with gentle cross-flow along positive Z-axis (middle). Experimentally measured directivity plots along the vertical (y-z) plane from a scale model in a wind tunnel (right). Adapted from Leav (2020, 2021).

This paper reports on field trials conducted on a small scale 250kW open cycle gas turbine, and aims to quantify the refraction of sound radiated from the exhaust. The paper is structured as follows: in Section 2, the details of the experimental configuration and measurement systems are provided; in Section 3, the results of the acoustic measurements from fixed microphone arrays, roving microphones and acoustic cameras are presented; in Section 4, the results are summarised and related to ISO 9613-2:1996 and CONCAWE, with guidelines for acousticians on how to predict far-field sound pressure levels (SPLs) from OCGT power stations.

2 EXPERIMENT DETAILS

This section details the experimental configuration, including the site, gas turbine, measurement equipment, and the operating conditions during tests.

2.1 Site details

All tests were conducted at The University of Adelaide's Buckland Park facility, approximately 40km north of the Adelaide CBD. The site and surrounding land is predominantly cleared agricultural land, with scattered vegetation (at the boundaries). The site arrangement is shown in Figure 2, which shows the position of the acoustically treated 20-foot modified shipping container that housed the gas turbine, the 100mm diameter exhaust stack that extended approximately 5m from the container at a height of 2m above the ground plane, along with the locations of a logarithmic microphone line array and two circular arc microphone arrays. The closest building (of dimensions 3m x 3m) was ~50m from the exhaust outlet. The arrangement of the exhaust stack and microphone arrays were chosen to align with the predominant wind direction, which is from the south-west. The temperature profile was relatively uniform from 1m up to 4m (the limit of measurements).

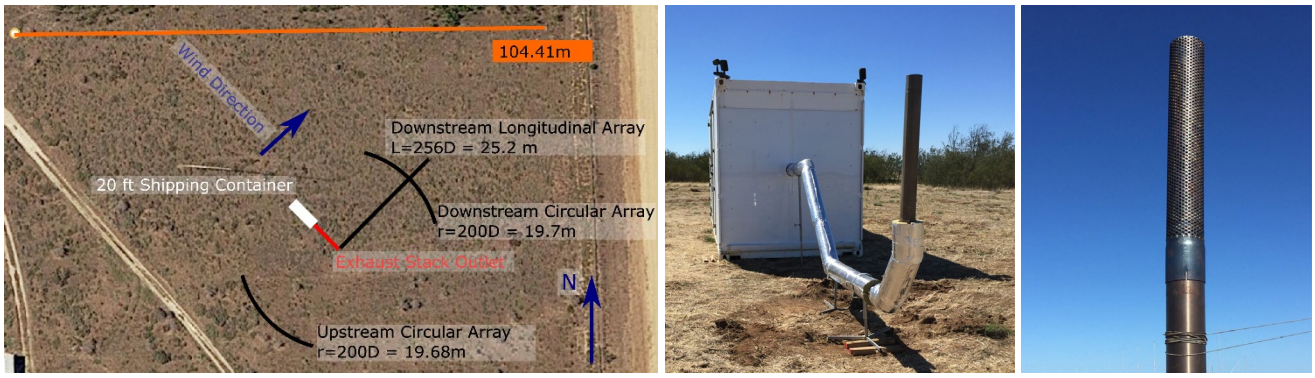

Figure 2: Aerial view of the test site, showing the shipping container, the exhaust stack, and the microphone arrays (left); photograph of the acoustically treated shipping container with lagged exhaust system (middle); acoustically transparent porous duct extension 6*D* long (right).

2.2 Gas turbine and exhaust system

The experiments were conducted on a Turbine Technologies SR-30 (Brayton cycle) turbojet engine, shown in Figure 3. The turbine was fitted with a HushKit inlet suppressor to reduce sound radiation from the intake and compressor stage, and the exhaust silencer was removed to increase the sound power transmitted to the stack. The turbine consists of a 12 bladed centrifugal flow compressor, annular combustor and axial flow power turbine (Turbine Technologies, 2007). The turbine has a compression ratio of 2.5:1, has a maximum mass flow rate of approximately 0.5kg/s, a maximum operating speed of 87,000RPM and a maximum exhaust gas temperature of 720°C. At maximum speed the turbine consumes ~6g/s of kerosene which is equivalent to 250kW of heat released.

Figure 3: Close up image of the SR-30 turbojet engine, showing the inlet HushKit, turbine and exhaust inlet (left); photograph of turbojet engine in the acoustically treated shipping container on startup (right).

The exhaust system comprised a *D*=100mm ID stainless steel duct, lagged with 50mm Roxul Stonewool Rock-Tech S 650 that extended for a length 7.65m, with the outlet 2m above the ground. The lagging (Figure 2) provided thermal and acoustic insulation.

2.3 Acoustic and flow measurements

The acoustic measurements were made using a variety of systems: fixed microphone arrays, a roving dual-input Sound Level Meter (SLM) and acoustic cameras. Additional measurements were made to measure the flow speed at the exhaust, and the wind speed and direction.

2.3.1 Fixed microphone arrays and DAQ

The fixed microphone arrays comprised two circular arcs spanning ±30°, with a radius of 20m which is equivalent to 200 exhaust diameters, *D*. Each circular microphone array had 13 microphones with an angular increment of 5°. A logarithmically spaced line array was installed, with six microphones spaced at 8, 16, 32, 64, 128 and 256 exhaust diameters, *D*, from the exhaust outlet. All fixed arrays were at approximately the same height as the outlet (2m above the ground) and used GRAS 40PH ¼" free field ICP microphones with windscreens. The arrays were constructed from purpose-built 25NB galvanised pipe, as shown in Figure 4. In addition to the microphone arrays, two additional 40PH microphones were used to measure the near-field SPL at a position of 5*D* and 8*D*. All array microphone signals were recorded at a sample rate of 25.6 kHz using a National Instruments PXIe-1073 chassis and NI PXIe-4499 DAQ cards. All microphones were calibrated with a Bruel and Kjaer 4231 with a ¼" adaptor. Data from each test was recorded for 120s.

Figure 4: Photographs of the "upwind" circular arc array (left); the "downwind" logarithmic line array (and "downwind" circular arc array) with the shipping container in the background (middle); the roving SLM with lower and upper microphones, the windsock streamer and the exhaust outlet and shipping container (right).

2.3.2 Roving SLM

A Bruel and Kjaer 2270 Sound Level Meter (SLM) was used to undertake roving SPL measurements at two heights: 1m and 3m, i.e., ±1m from the exhaust outlet plane. The lower microphone was a Bruel and Kjaer 4189 ½" free-field microphone, and the upper microphone was a GRAS 146AE ½" free-field microphone. Both were calibrated using a Bruel and Kjaer 4231 and fitted with windshields. Measurements were taken for 30s, and statistics such as Leq, L10, L90 were obtained for one third-octave bands as well as overall SPL.

2.3.3 Acoustic Cameras

Three acoustic cameras (shown in Figure 5) were used during the experiments: a portable SoundCam (supplied by Resonate Consultants) comprising 64 microphones, with a 300mm aperture sampled at 48kHz with 24-bit precision providing a recommended operating range above 800Hz; and two gfai tech 48 element acoustic cameras (supplied by HW Technologies): (1) a Ring48 AC Pro ring array with an aperture of 750mm and recommended operating frequency range of 164Hz-20kHz, and (2) a Star48 AC Pro star array with an aperture of 3400mm with recommended operating frequencies from 66Hz-13kHz, with data recorded on a gfai-tech data recorder 721B. Since all cameras were on loan, they were only available for a limited number of measurements.

2.3.4 Flow measurements

Flow measurements comprised of turbine data, exhaust temperatures, exhaust flow rate, wind speed, and wind direction. The turbine data included rotational speed in RPM and exhaust gas temperature, and was obtained from the control panel of the SR-30. Three k-type thermocouples attached to the exhaust system were used to measure the inlet temperature, gas turbine exhaust temperature and the temperature of the exhaust outlet. These were logged using the NI PXIe system simultaneously with the array microphone signals. The wind was measured

by a RISO P2546A anemometer and an R.M. Young Model 81005A three-axis ultrasonic anemometer, which provided both wind speed and wind direction. The analog signals from the two anemometers were recorded using a NI-PXI 6221, with a sampling frequency of 25.6 kHz. At the end of each run, the exhaust flow speed was measured using a Fluke 922 flow meter and a Testo high temperature Inconel pitot-tube.

Figure 5: Photographs of the acoustic cameras used to visualise the sound field. Left-hand image is the portable SoundCam (kindly supplied by Resonate Consultants) with compression driver on the stack; and the right-hand image shows the gfai tech Ring48 and Star48 acoustic cameras (kindly supplied by HW Technologies).

3 RESULTS

This section details the test configurations and the results obtained.

3.1 Test configurations

The turbine was operated under two general conditions: low speed just above idle at approximately 45,000RPM, with an exhaust flow at the outlet of Mach $M_j = 0.06$ and temperature $T_j = 400°C$; and high speed at approximately 75,000RPM, with an exhaust flow at the outlet of Mach $M_j = 0.12$ and temperature $T_j = 550°C$. These were taken under numerous meteorological conditions from calm (~1m/s) to 8m/s. Two stack outlet arrangements were investigated; a hard walled outlet shown in Figure 2 (middle); and an acoustically transparent duct extension of 600mm, built from 50% open area perforated plate and lined internally with a stainless woven cloth (Figure 2, right). This extension forces the flow to vent 6D above the measurement plane, but permits the sound to radiate from the measurement plane. The insertion loss of transparent extension in the frequency range of interest was measured in a reverberation chamber to be ≤2dB. The normal incidence transmission loss was <2dB.

3.2 Acoustic cameras

The acoustic cameras were used to assist in locating the dominant noise sources across the frequency range of interest as well as visualise the sound field. In all the measurements, the exhaust outlet dominated the frequency range of interest by at least 20dB. The three images in Figure 6 are the sound fields observed from the gfai tech ring array at a Helmholtz frequency of approximately ka=1 (~1800Hz, where the radius a=D/2). What can be observed is that the reference sound source (a large compression driver with an outlet diameter of 50.8mm) produces a spherical radiation pattern in Figure 6 left (circular when projected on the image plane), acting like a monopole as expected. However, the sound radiation pattern from the hot exhaust stack when viewed from downwind is elliptical (Figure 6 middle), and somewhat similar to a finite line source, and is very different than would be observed from a duct radiating below cut-on in the absence of heat or flow. The observed sound field was found to be quite unstable, with large “bubbles” of sound being refracted downwind to the receiving array as observed in Figure 6 right. These results are consistent with the earlier work of Leav et al. (2017, 2018, 2021), which predicted the source would not appear as a monopole when observed from the geometric far-field, but rather a source extended in the vertical axis like a finite line source.

3.3 Fixed microphone arrays

The fixed microphone arrays permitted instantaneous sampling of the soundfield. The logarithmic array line was useful for quantifying the attenuation due to distance, typically assumed to be -6dB/doubling of distance when in the far-field. The circular arrays permitted the characterisation of the angular directivity. The arrays were also used to assess the temporal variability using statistics such as L10 and L90.

3.3.1 Spreading rates versus distance

Figure 7 shows plots of the Leq (120 seconds) versus distance from the source for three cases: the compression driver used as a (monopole) reference source measured downwind; the hard exhaust stack (operating at 45,800 RPM) measured upwind; same hard configuration (operating at 43,800 RPM) measured downwind. The compression driver SPLs were also measured upwind, exhibiting thesame results as downwind. It can be seen that the SPL downwind of the compression driver and the SPL upwind of the hard exhaust stack both show trends consistent with spherical spreading, as would be expected at these frequencies. The ground surface was soft, lose soil covered in grass, hence reflections were negligible for the frequency range. The deviation from spherical spreading at 256*D* for 1600Hz was due to background noise. However, the SPL measured downwind from the hard stack does not follow conventional spherical spreading, i.e., 6dB reduction in SPL for each doubling in distance. Rather it attenuates at -4.8dB/doubling of distance and sits somewhere between a point source (-6dB) and a line source (-3dB). These geometric spreading rates are for 120s of data. Much more pronounced deviations from -6dB/doubling were seen for durations shorter than 120s. Durations greater 120s the SPLs had stabilised. Atmospheric refraction and convection effects were negligible over the tested distances and momentum ratios.

Figure 6: Acoustic field observed by the 48 microphone gfai tech ring array: compression driver reference sound source SPL 1.6kHz third-octave (16s) (left), hot exhaust stack with the turbine operating at 43,800 RPM SPL 1.6kHz third-octave (32s) (middle); and “bubbles” of sound observed from turbine (43,800 RPM) when wind gusts are present SPL 1kHz octave (1s) (right). All images are taken downwind for a dynamic range of 10dB.

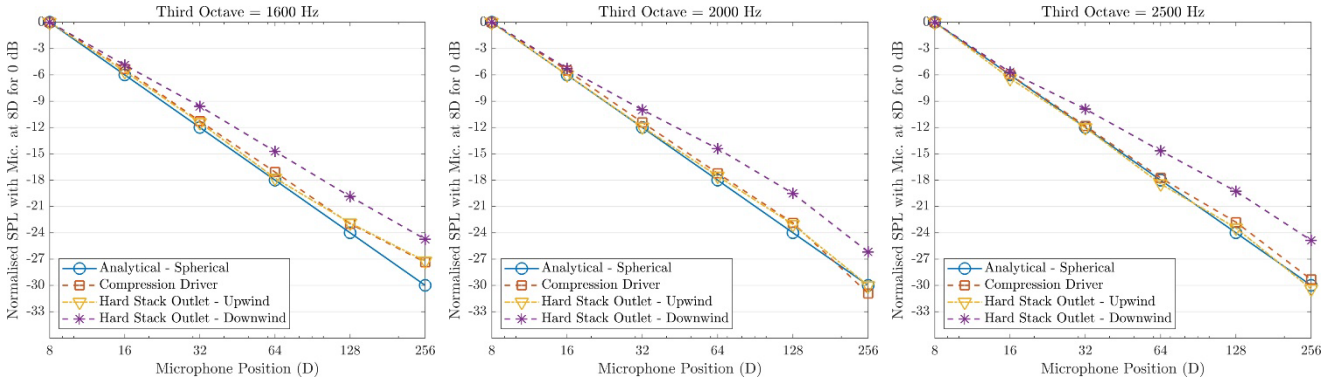

Figure 7: Sound pressure level Leq (duration 120s) for third-octave bands 1.6kHz, 2kHz and 2.5kHz, measured by the logarithmic line array normalised to 0 dB versus distance normalised by the exhaust diameter, *D*, compared to -6dB/doubling (spherical spreading): compression driver mounted on top of the exhaust outlet, hard stack outlet upwind (1.6-3.9 m/s), hard stack outlet downwind (3.8-7.3 m/s).

3.3.2 Sound directivity

Figure 8 plots the Leq (120s) from the upwind and downwind circular array microphones, with the turbine operating at 43,800RPM configured with the hard exhaust stack, showing three third-octave bands just below cut-on. It can be seen that a strong lobe is observed in the downwind direction at the outlet plane of the exhaust. The SPL difference between downwind and upwind is ~8 dB, 7 dB, and 9 dB for 1.6 kHz, 2 kHz, and 2.5 kHz third octave bands, respectively. Both the width and magnitude of the downwind lobe were very sensitive to wind direction and exhibited strong temporal variability. Though not presented here, when the Leq was calculated over shorter time frames (15-30s) the peak in the downstream lobe was observed to be up to 12-15dB higher than upwind.

3.3.3 Temporal variability

As previously indicated, the downwind SPLs were quite unstable and showed strong dependence on wind direction and speed. To illustrate this, the difference between L10-L90 statistic is shown in Figure 9 (using the same

dataset plotted in Figure 8). It shows that upwind of the exhaust outlet, the SPL is stable; however, the downwind SPL fluctuates significantly due to the interaction of the sound through the plume. Figure 10 shows the SPL (1s intervals) in the 1.6kHz third-octave band is presented versus time for the microphone directly downwind and upwind . The difference between L10 and L90 was typically 8-10dB downwind, which quantifies the high variability in sound levels, whereas upwind it was typically 2-4dB, suggesting the upwind sound levels are relatively stable compared with downwind levels.

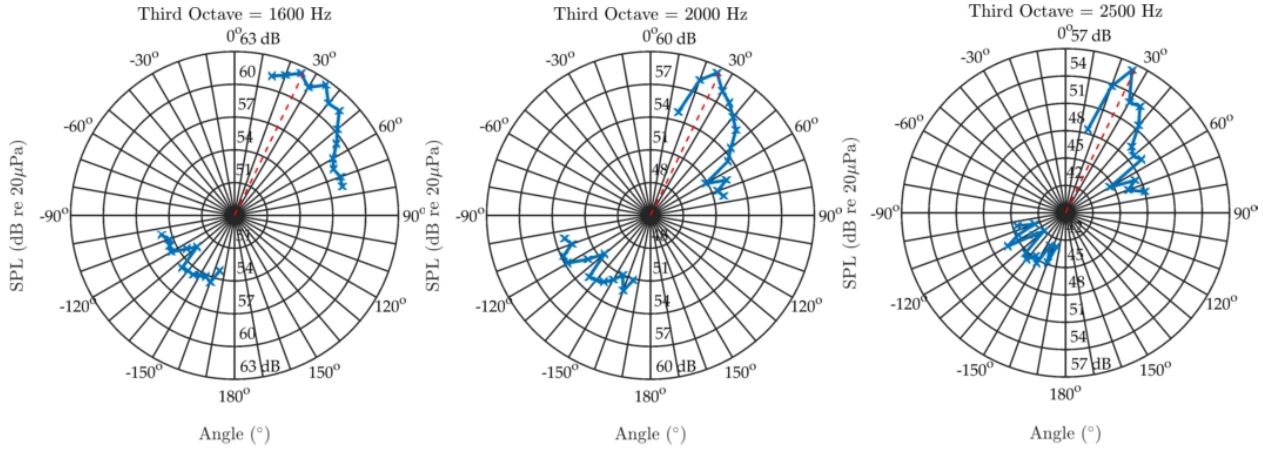

Figure 8: Sound pressure level Leq over 120s from circular microphone arrays. The turbine speed was 43,800RPM. Red line indicates downwind direction.

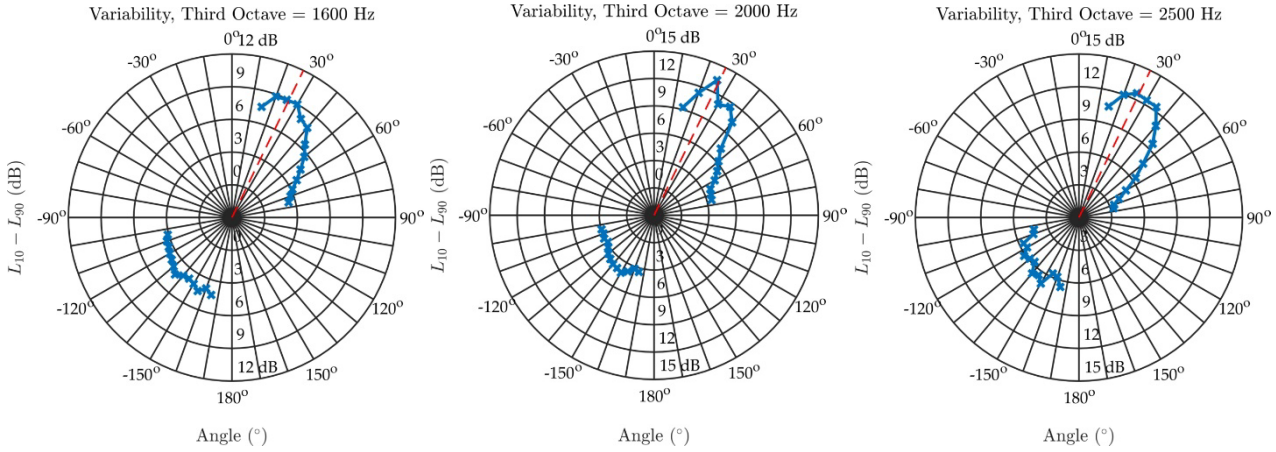

Figure 9: L10-L90 statistic over 120s from circular microphone arrays, which provides a measure of temporal variability. The turbine speed was 43,800RPM. Red line indicates downwind direction.

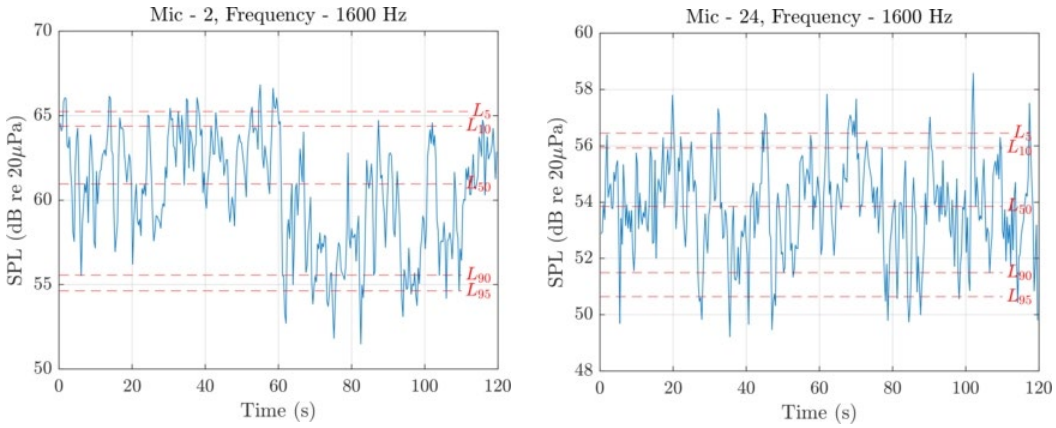

Figure 10: Microphone SPL in 1s periods for microphones directly downwind (mic 2) and upwind (mic 24) 120s. Turbine speed 43,800RPM.

3.4 Roving SLM

The SLM was used to measure the SPLs (1m) below and (1m) above the plane of the exhaust outlet, and because of the portability, permitted measurements that were guaranteed to be downwind, unlike the fixed arrays. Figure 11 presents these measurements downwind of the stack at a distance of 64*D* (6.4m) from the outlet. The SPLs above the outlet plane were found to be 3-8dB higher than below. The other interesting point to note is that the acoustically transparent duct extension leads to a very significant reduction in the SPLs, especially for the upper microphone which is closer to the peak in the lobe (as seen in Figure 1). This reduction in SPL is achieved almost entirely through modification of the sound refraction, by separating the acoustic field and the flow field, with only 2dB associated with IL of the extension.

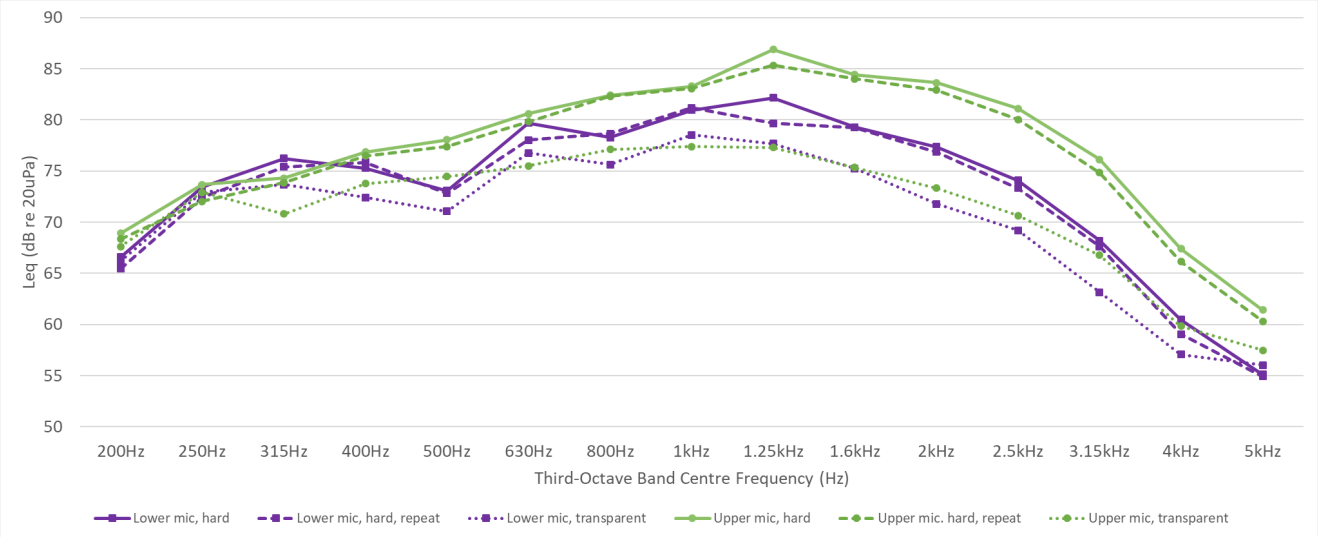

Figure 11: SPL Leq (30s) at a distance of 64*D* downwind of the exhaust outlet with the turbine operating at 75,000RPM, measured 1m below and 1m above the exhaust outlet (lower and upper mic). There were three configurations: two hard walled stacks (to demonstrate repeatability), and one with the transparent extension.

4 DISCUSSION AND APPLICATION TO OPEN CYCLE GAS TURBINE

The results detailed above have implications for estimating SPLs from gas turbines, such as in the case of open cycle power stations, and gas turbine driven gas pumping and compressor stations. Since the non-dimensional parameters for the study are the same as found in larger gas turbines (Mach number, jet to ambient temperature ratio, momentum cross-flow ratio, Helmholtz number, and distance to diameter ratio), with only the Reynolds number differing, the same behaviour in downwind SPLs are expected to be observed for larger turbines, which typically have exhaust diameters from 2-6m (i.e. 20-60 times larger). Sound pressure levels at far-field receivers are often predicted using ISO 9613-2:1996, and CONCAWE is used to account for atmospheric refraction. For example, consider a gas turbine with a 5m diameter exhaust. The distances out to which measurements were made here are equivalent to 256*D* = 1.28km, which is similar to the distances accommodated by CONCAWE, which was developed from measurements taken around petrochemical complexes (including furnace exhausts and boilers). Using Meteorological Criteria 6, the meteorological corrections (Simplification 2) for octave bands from 250Hz to 4kHz is approximately 5dB and decreases approximately linearly towards 31.5Hz. This represents the most likely outcome. However, it was reported that there was significant variance, and to provide an estimate of upper bound SPL with 97.5% confidence, another 5-10dB must be added. Thus, the upper bound on the meteorological correction becomes 10-15dB for the most adverse conditions. This is consistent with the levels reported in Section 3, and is consistent across frequencies once scaled.

It is not clear how much refraction continues beyond the distances measured here. It is well known that atmospheric turbulence plays an important role in degrading the coherence of the sound field at larger distances. This was observed during these trials, where close to the source the SPLs were stable, and the opposite occurred at distances far from the source. This implies that temporal variability increases as distance increases, and thus whilst the average SPLs might be lower, the resulting intermittency could lead to increased annoyance in a nearby community, thus possibly offsetting any reduction in SPL due to loss of coherence. Further research is required to understand how the localised refraction in the plume is compounded by atmospheric refraction, but it is expected that both phenomena will lead to increased levels.

5 CONCLUSIONS

The work presented in this paper clearly shows that sound radiation from hot exhaust stacks is heavily affected by local refraction as the sound propagates from the outlet through the plume. In the presence of gentle cross-wind, downwind SPLs in the far-field for octave bands at *ka*=1 could be up to 10-12dB higher than predicted using a monopole source with spherical geometric spreading, even below the cut-on frequency of higher order modes in the duct. The downwind sound levels were found to be very unstable and strongly dependent on wind direction and wind gusts. Comparisons were made with predictions from CONCAWE under adverse meteorological conditions, with the current results mirroring the levels observed in the CONCAWE uncertainty data. The paper definitively demonstrates increased downwind SPLs from hot exhaust systems will be observed at sensitive receivers well beyond the levels (most likely) predicted using ISO 9613-2 or CONCAWE. Acousticians and planners should consider the likelihood of this phenomenon occurring in the planning and design stages for open-cycle gas turbine installations.

ACKNOWLEDGEMENTS

The authors gratefully acknowledge the Australian Acoustical Society for the Research Grant which supported this research. The provision of acoustic cameras and technical support from Resonate Consultants and HW Technologies is also gratefully acknowledged. We also acknowledge the support of Ilse Scharfbillig for access to the test site, Rob Dempster in commissioning the turbine, Phanh Nieng and Alecia Leav for their support in construction of the fixed arrays and to Virak and Linda Khath for emergency use of their air compressor.

REFERENCES

Björk, E. (1994). “Experimental study of measures to reduce noise radiated from power-station exhaust stacks,” Noise Control Eng. J. 42, 171–178. https://doi.org/10.3397/1.2828354

Broner, N. (2010). “A simple criterion for low frequency noise emission assessment,” J. Low Freq. Noise Vib. Active Control 29, 1–13. https://doi.org/10.1260/0263-0923.29.1.1

Broner, N. (2011). “A simple outdoor criterion for assessment of low frequency noise emission,” Acoustics Australia, 39, 7–14.

Broner, N. (2012) “Power to the people,” in Proceedings of the 15th International Meeting on Low Frequency Noise and Vibration and Its Control, Stratford upon Avon, United Kingdom (May 22–24, 2012), pp. 1–10.

Hessler, G., Jr. (2004). “Proposed criteria in residential communities for low-frequency noise emissions from industrial sources,” Noise Control Eng. J. 52, 179–185. https://doi.org/10.3397/1.2839748

Hessler, G., Jr. (2005) “Proposed criteria for low frequency industrial noise in residential communities,” Low Freq. Noise Vib. Active Control 24, 97–106 (2005). https://doi.org/10.1260/0263092054530957

Hetzel, R. and Putnam, R. (2009). “Sources and rating criteria of low frequency gas turbine exhaust noise—Via case study,” in Proceedings of INTER-NOISE and NOISE-CON, Ottawa, Canada, pp. 1600–1607.

ISO 9613-2:1996: Acoustics—Attenuation of Sound During Propagation Outdoors—Part 2: General Method of Calculation (ISO, Geneva, Switzerland, 1996).

Kudernatsch, G. (2000). “Combustion turbine exhaust systems-low frequency noise reduction,” in Proceedings of INTER-NOISE 2000, Nice, France (August 27–31, 2000), pp. 1–6.

Leav, O.Y.J., Cazzolato, B.S. and Howard, C.Q. (2021). “Sound propagation through elevated, heated jets in cooler cross-flow: An experimental study”, JASA, 150 (1), pp 82-93. https://doi.org/10.1121/10.0005489

Leav, O.Y.J. (2020). “An investigation into the mechanics of sound propagation through turbulent non-isothermal exhaust jets in cross-flow”, PhD thesis, University of Adelaide, Adelaide.

Leav, O.Y.J., Cazzolato, B.S. and Howard, C.Q. (2018). “Experimental analysis of sound directivity from sound propagation through non-isothermal, turbulent exhaust jets in cross-flow”, in Proc. Australian Acoust. Society.

Leav, O.Y.J., Cazzolato, B.S. and Howard, C.Q. (2017). “A computational analysis of sound directivity from sound propagation through non-isothermal, turbulent exhaust jets in cross-flow,” in Proc. 24th ICSV, London, UK.

Lucas, W.C. and Hessler, G.F., Jr. (1996). “The reduction of low frequency gas turbine exhaust noise: A case study,” in ASME 1996 International Gas Turbine and Aeroengine Congress and Exhibition, Turbo Expo: Power for Land, Sea, and Air, Birmingham, UK (June 10–13, 1996).

Manning, C.J., (1981). “The propagation of noise from petroleum and petrochemical complexes to neighbouring communities”, AT 931, Acoustic Technology Limited, for CONCAWE, Report no. 4/81.

Newman, J.R. and McEwan, K.I. (1980). “Low frequency gas turbine noise,” J. Eng. Power 102, 476–481. https://doi.org/10.1115/1.3230280

Turbine Technologies, MiniLab Gas Turbine Power System Operator's Manual, Model ML-401, REVISION 7/06 (1.21)

Zaporozhets, O., Karpenko, S., and Levchenko, L. (2021). Calculation tool NoBel for sound propagation assessment of noise from gas turbines on the ground, Proc. InterNoise 2021. https://doi.org/10.3397/IN-2021-2717